

## **Salt Crystallization in Hydrophobic Porous Materials**

**H. Derluyn<sup>1</sup>, A.S. Poupeleer<sup>1</sup>, D. Van Gemert<sup>1</sup> and J. Carmeliet<sup>1,2</sup>**

<sup>1</sup>Department of Civil Engineering, Katholieke Universiteit Leuven, Heverlee, Belgium

<sup>2</sup>Faculty of Building and Architecture, Building Physics and Systems, T.U. Eindhoven, The Netherlands

### **Abstract**

This paper presents the results of drying experiments on hydrophobized calcium silicate (*ca/silb*) beams in order to validate theoretical models describing salt transport and salt crystallization. Experimental data include results from moisture transport as well as deformation measurements of the beams. X-ray analysis is used to determine the moisture transport, SEM and EDX to localize and analyze the salt crystals. The performed experiments validate a crystallization model that was developed recently by Coussy. They also validate the poromechanical interpretation of the mechanical behaviour of the beams when influenced by the presence of moisture and salt crystals. A good agreement between measurements and modelling is obtained.

**Keywords:** salt damage, salt decay, crystallization, poromechanics, hydrophobic treatment.

## 1 Introduction

The hygric and mechanical behaviour of porous materials is significantly influenced by any moisture and contaminating agents they contain. When salts are dissolved in water that is absorbed by the material, they will crystallize as the material dries out. Crystallization inside the porous structure induces expansive forces in the material that can eventually lead to damage and cracking.

In the relevant literature various experiments are described intended to measure salt transport and salt crystallization [1-3]. Apart from measurements, modelling approaches for transport and crystallization processes have been developed. A finite element model for heat, mass and salt transport was developed by Koniorczyk and Gawin [4]. A model based on controlled volume was developed by Poupeleer [5]. Recently, a crystallization theory based on thermodynamics was developed by Coussy [6]. By the theory of poromechanics, the mechanical behaviour of porous materials can be modelled (Coussy [7]).

The first part of this paper describes drying experiments on hydrophobized calcium silicate beams. The second part uses these results to validate both the crystallization and the poromechanical model.

## 2 Experimental work

Hydrophobized calcium silicate beams were subjected to drying at constant relative humidity (RH) of 54% and temperature of 23°C after saturation with water or an aqueous 1M Na<sub>2</sub>SO<sub>4</sub> solution. The experiments aim to investigate the four aspects of the drying process: (1) change in moisture content; (2) salt transport and salt crystallization in the material; (3) shrinkage due to drying and expansion due to salt crystallization; and, (4) occurrence of damage.

### 2.1 Material properties

A calcium silicate insulation board, *calsilb*, was used for the experiments because it is a homogenous and isotropic porous material. It has a total porosity of 89.4% as determined by vacuum saturation with distilled water. It has mostly coarse pores (see Figure 1) as determined by Mercury Intrusion Porosimetry (MIP). *Calsilb* has a density of 270 kg/m<sup>3</sup> and a maximum capillary water uptake of 812 kg/m<sup>3</sup>; this value equals the area of the pore volume distribution curve of the capillary saturated material in Figure 1. The E-modulus, determined by a compression test, is 436 MPa for dry *calsilb*, and 291 MPa for water saturated *calsilb*. Its tensile strength is 0.3 MPa.

The water repellent product is the micro-emulsion SILRES BS SMK 1311 based on silanes and oligomer siloxanes.

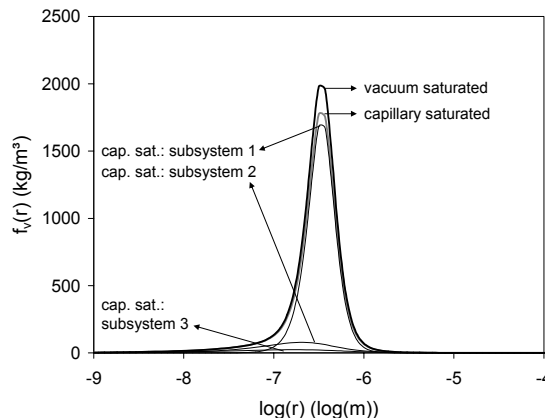


**Figure 1:** Pore volume distribution reached in capillary and vacuum saturated condition in function of pore radius.

The physical properties, i.e., high porosity, high capillary moisture content, low stiffness and strength, together with the application of the hydrophobic treatment make this material very useful for crystallization experiments. In the case of untreated *calsilb*, any salts present in it will be transported to the outer surface of the sample during drying and result in efflorescence. When a water repellent is applied, the salts will precipitate in the material because the hydrophobic zone at the outer surface prevents liquid water transport to the surface. The precipitation of the salts will induce stresses in the material resulting in measurable expansion and damage.

## 2.2 Measuring principles and measurement data

### 2.2.1 Sample preparation

The samples are beams of 30 x 70 x 200 mm<sup>3</sup> sawn in dry conditions out of a *calsilb* board. The lateral sides were coated with vapour tight paint to avoid evaporation. The hydrophobic treatment was applied by capillarity for one second in two consecutive times (2 x 1s) to the front surface (see Figure 2). Then, the specimen was submitted to capillary absorption at constant temperature by placing the back surface in contact with either water or an aqueous 1M Na<sub>2</sub>SO<sub>4</sub> solution until the specimen was saturated by capillarity. Immediately upon completion of the absorption process, the wet back surface was sealed with a silicone water tight material so as to obtain a one dimensional drying process through either the untreated or the water repellent treated surface.

In total, four samples were prepared, two for the water tests and two for the salt solution. For each of these, one sample was used to determine the change in moisture content and the other one to measure the deformation.

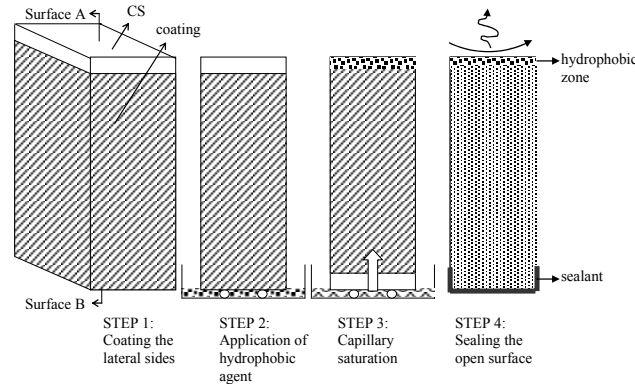


**Figure 2:** Preparation of the test samples.

### 2.2.2 X-ray analysis – moisture content

The evolution of moisture content in time was determined by X-ray imaging [8]. This technique enables a visualization of the interior of non-transparent objects in a non-destructive way. To visualize the moisture content, the image of the dry sample is subtracted from that of the wet sample. The moisture content is calculated based on the transmitted X-ray intensities.

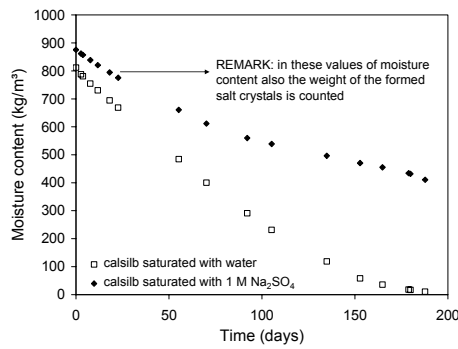


**Figure 3:** Isohygrothermal drying of saturated *calsilb* using distilled water and 1M Na<sub>2</sub>SO<sub>4</sub> (54% RH, 23°C).

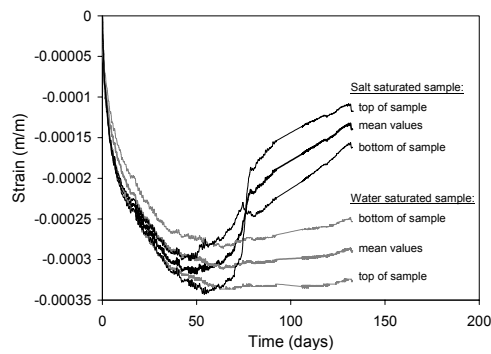


**Figure 4:** Deformation of the drying *calsilb* samples saturated with distilled water and with 1M Na<sub>2</sub>SO<sub>4</sub> solution.

The decrease in average moisture content during drying is shown in Figure 3. As expected the sample saturated with the salt solution dried slower than that saturated with water. The initial moisture content at the start of the drying process is higher for the sample saturated with salt solution due to the difference in density of the saturation solutions (at 23°C:  $\rho_{\text{salt solution}} = 1111.3 \text{ kg/m}^3$ ,  $\rho_{\text{water}} = 997.5 \text{ kg/m}^3$ ).

### 2.2.3 Deformation measurements

Shrinkage due to drying and expansion resulting from salt crystallization is measured by LVDTs (Linear Variable Differential Transformers), with a measuring range of 0 to 2000  $\mu\text{m}$  and a resolution of 0.12  $\mu\text{m}$ . The back side of the specimen is fixed, while the displacements of the front surface where drying takes place is measured.

The measured deformations are shown in Figure 4. The strains  $\varepsilon$  are related to the initial length of the saturated sample. First, shrinkage due to drying is observed for both samples. After a certain time, expansion starts to occur in the salt saturated sample as crystallization occurs at the limited transition zone between the untreated part and the hydrophobized surface layer. Finally, after approximately 80 days, a crack is formed at this interface after which salts crystallize freely at the surfaces of the crack.

### 2.2.4 SEM and EDX analysis

The location of the precipitated salt was analyzed by SEM analysis (Scanning Electron Microscope). Additionally, EDX (Energy Dispersive X-ray) analysis was performed for element characterization. As described above, precipitated salt crystals are localized in the transition zone between non-hydrophobic and hydrophobic material. SEM-analyses were carried out on specimens taken from 5 different locations with regards to the transition zone (Figure 5):

- (1) Position 1: in the untreated zone at 1.5 cm left of the transition line;
- (2) Position 2: around 1 cm left of the transition line;
- (3) Position 3: at the transition line between hydrophobic and non hydrophobic material;
- (4) Position 4: located in the hydrophobic layer around 0.2 mm right of the transition line;
- (5) Position 5: located in the hydrophobic layer at 0.8 cm right of the transition line.

It is to be pointed out that the transition between the untreated zone and the hydrophobic layer is not a straight line, as can be seen on the X-ray image in Figure 5. However, for simplification in the subsequent analysis, the transition will be considered as a line.

EDX-analysis at position 1, in the non treated zone, shows mainly Ca and Si. Only in some distinct places, a limited amount of precipitated  $\text{Na}_2\text{SO}_4$  is found. At position 2, closer to the drying front, the amount of salt is higher than at position 1. At position 3, where the cracked surface is, the whole area is covered by precipitated salts. At position 4, in the hydrophobic zone at the right side of the drying front, also spots with a high salt amount are detected. Finally, at position 5 further away from the transition line into the hydrophobic zone, no salts were detected.

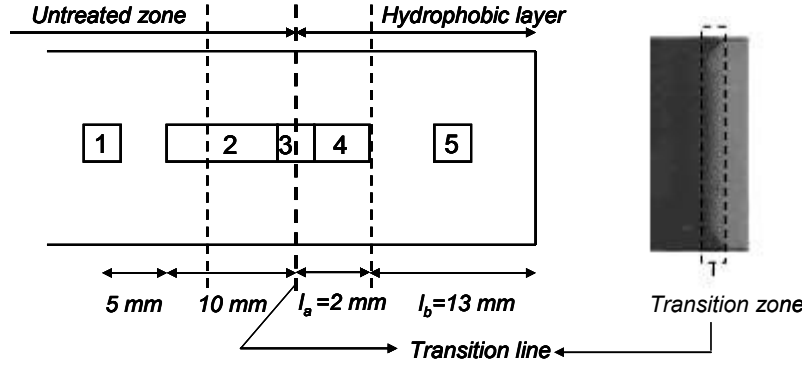


**Figure 5:** Schematic indication of the analyzed positions of the sample initially saturated with 1M Na<sub>2</sub>SO<sub>4</sub>.

Concluding, it can be stated that salt crystals are not only formed in the untreated zone close to the drying front, but also in part of the hydrophobic layer close to the transition line. The analysis shows an infiltration of salt crystals in the hydrophobic zone over a distance of 2 mm.

### 3 Modelling

To cover all processes acting in a salt loaded porous material, a model consisting of three main parts was developed:

- (1) a model for heat, moisture and salt transport [5];
- (2) a crystallization theory based on thermodynamics [6];
- (3) a poromechanical model [7].

In this section, a closer look is taken at part (2) and (3). Finally, the simplified modelling of the hydrophobic layer is also described.

#### 3.1 Salt crystallization

A thermodynamic approach, based on the work of Coussy [6], is used to describe the crystallization process. Crystallization conditions are deduced based on the balance between salt solution - salt crystal. These conditions depend on the relative humidity, the supersaturation and the salt characteristics.

The overall equations expressing the crystallization conditions are:

$$\left( \frac{\Phi}{1 - Nx^*} \right)^{\frac{v_x}{v_w} \left( \frac{\gamma_{sl}}{\gamma_{gl}} + \delta \right)} \left( \frac{x^*}{x_0} \right)^N \left( \frac{1 - Nx^*}{1 - Nx_0^*} \right)^{v_w} = 1 \quad (1)$$

$$\frac{1}{r} = \frac{RT}{2v_x(\gamma_{xl} + \delta\gamma_{gl})} \ln \left[ \left( \frac{x^*}{x_0^*} \right)^N \left( \frac{1 - Nx^*}{1 - Nx_0^*} \right)^{v_w} \right] \quad (2)$$

where  $\Phi$  is the relative humidity,  $x^*$  is the molar fraction for crystallization at this relative humidity and  $x_0^*$  is the molar fraction at  $\Phi = 1$ .  $N$  is the sum of the stoichiometric coefficients of the salt ions and  $v_w$  is the stoichiometric coefficient of water.  $v_w$  is the molar volume of water,  $v_x$  the molar volume of the salt crystal.  $\gamma_{xl}$  is the interfacial energy between the salt crystal and the salt solution,  $\gamma_{gl}$  the interfacial energy between the salt solution and the gas phase.  $\delta$  is a dilation coefficient, accounting for the volume change resulting from the crystallization process.  $r$  represents the pore access radius related to the crystallizing pores.

With decreasing relative humidity  $x^*$  increases. The ratio between  $x^*$ , the molar fraction for crystallization at this relative humidity, and  $x_0^*$ , the molar fraction at  $\Phi = 1$ , is called the supersaturation degree.

At a certain relative humidity, crystallization takes place. By recalculating molar fractions in (1) to salt concentrations, this process will occur when the salt concentration  $C_s$  exceeds the saturated salt concentration  $C_{s,sat}$ . Assuming no transition kinetics for the crystallization reaction, the general condition for salt crystallization is stated as:

$$IF C_s > C_{s,sat} THEN C_s = C_{s,sat} \text{ and the residue precipitates} \quad (3)$$

Then from (2) the corresponding access pore radius for salt crystals can be calculated. This means that crystals can grow in pores with a pore radius larger or equal to  $r$ . Thus crystallization first occurs in the largest pores during drying and eventually also in the smaller pores.

### 3.2 Poromechanics: deformations

To incorporate the influence of the pore fluid and the salt crystals on the mechanical behaviour of the porous material, the theory of poromechanics as developed by Coussy [7] was used. Both liquid as well as formed crystals present in the matrix can introduce pressures on the pore walls. For an open porous medium the isotropic constitutive equation for isothermal conditions becomes:

$$\sigma = C\varepsilon - b_l \int_{p_c} S_l(p_c) dp_c \mathbf{I} - b_x \int_{p_x} S_x(p_x) dp_x \mathbf{I} \quad (4)$$

where  $\sigma$  is the stress tensor,  $\varepsilon$  is the strain tensor,  $C$  is the elastic isotropic constitutive tensor,  $b_l$  is the Biot or coupling coefficient for liquid and  $b_x$  the Biot coefficient for salt;  $S_l(p_c)$  is the degree of moisture saturation in function of the capillary pressure and  $S_x(p_x)$  the degree of crystallization in function of the crystal pressure;  $\mathbf{I}$  is the second order unity tensor. The first term on the right hand side describes the stress contribution of elastic strains. The second term describes the influence of capillarity effects and the third term the influence of crystal pressures.

As the samples in the performed experiment can deform freely, no external stress is exerted. Therefore, the 1D strain can be calculated by:

$$\varepsilon_{tot} = \varepsilon_{liquid} + \varepsilon_{salt\ crystal} = \frac{(1-2\nu)}{E(S_l)} b_l \int_{p_c} S_l(p_c) dp_c + \frac{(1-2\nu)}{E(S_l)} b_x \int_{p_x} S_x(p_x) dp_x \quad (5)$$

where  $E(S_l)$  is the Young's modulus as a function of the saturation degree and  $\nu$  is the Poisson's ratio. It was assumed that the Young's modulus is independent of the crystallization degree  $S_x$  and that the coupling coefficients  $b_l$  and  $b_x$  are equal. The crystallization degree and the coupling coefficients were taken from Poupeleer [5].

### 3.3 Hydrophobic layer

The hydrophobic layer, having a length  $l_h$ , is considered as a resistance and is combined with the surface boundary coefficients of the environment. Therefore, the effective surface heat transfer coefficient  $\alpha_{eff}$  and effective surface mass transfer coefficient  $\beta_{eff}$  are described as follows:

$$\alpha_{eff} = \frac{1}{\frac{1}{\alpha} + \frac{l_h}{\lambda}} ; \quad \beta_{eff} = \frac{1}{\frac{1}{\beta} + Z_h \cdot \frac{l_b}{l_h} + Z_h \cdot \frac{l_a}{l_h} \frac{1}{\zeta_p}} \quad (6)$$

where  $\alpha$  and  $\beta$  are the transfer coefficients of the environment.  $Z_h$  is the vapour resistance of the hydrophobic layer and  $\lambda$  the thermal conductivity.  $l_b$  is the thickness of the hydrophobic zone without crystals (Figure 5).  $\zeta_p$  represents the fraction of open pores in the hydrophobic zone  $l_a$  where crystals are formed, in relation to the initial total porosity.

## 4 Results

The simulated drying curve of the salt loaded samples during the first 80 days, taking into account the porosity change of the hydrophobic layer due to crystallized salts, is plotted in Figure 6 (thin line). If the results are corrected for the weight increase of the formed crystals, the resulting simulated drying curve (thick line in Figure 6) matches well with the experimental curve. It is to be noted that even after 80 days a lot of liquid water remains in the smallest pores of the system.

The simulation curves for the deformation are represented in Figure 7, combining the shrinkage effect due to drying and the expansion effect due to crystal growth. A good agreement is obtained with the measured data; the jump in the curve going from shrinkage to expansion can be simulated accurately. Note that after the occurrence of the crack a comparison of the simulated and measured data is no longer meaningful.



In order to determine the fraction of open pores  $\zeta_p$  (in relation to the initial porosity) in the part of the hydrophobic layer where crystallization takes place, a distribution key for the salt crystallization is determined. The distribution is based on the measurements from SEM examination showing that:

- 15% precipitates in the hydrophobic zone
- 85% precipitates in the non hydrophobic zone.

By this distribution the fraction of open pores decreases during the drying of the sample and includes the formation of salt crystals in the hydrophobic zone. From (6), it follows that the mass transfer coefficient  $\beta_{eff}$  decreases. By this, the slower drying rate of the salt saturated sample is adequately modelled.

This salt crystallization distribution key shows that salts preferentially grow in the non-hydrophobic zone. A part of the crystals will also grow inside the hydrophobic zone since there is place available in the pores and because it is possible that the hydrophobic layer is not uniform and some salt solution may penetrate that zone. The effort to grow inside these pores seems more important. This could be based on changed surface tension and contact angle of the interface between solid crystal/liquid. The determination of the value of the salt crystallization key may seem arbitrary. However, the same distribution gives good results both for the simulation of the drying as for the deformation behaviour.

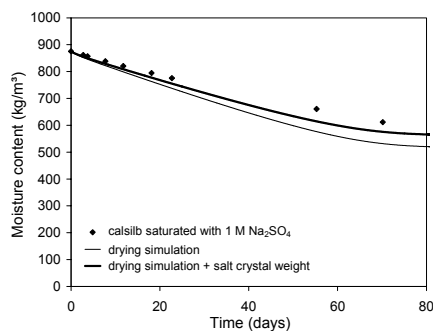


**Figure 6:** Experimental and numerical results of drying of salt saturated calsilb.

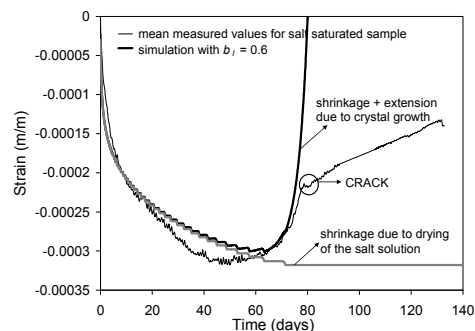


**Figure 7:** Experimental and numerical result of deformation of salt loaded calsilb.

## 5 Conclusions

The drying of a 1M  $\text{Na}_2\text{SO}_4$  saturated porous building material (calcium silicate board) treated with a water repellent under constant boundary conditions is presented. Not only mass transport, but also shrinkage due to drying and expansion due to salt crystallization were measured. For the complex modelling a coupled heat, moisture and salt model is developed. A crystallization criterion is formulated based on Coussy [6]. The strains

are modelled using a poromechanical approach. A good agreement between measurement and modelling suggests the ability of this approach to model adequately the different phenomena such as moisture transport, salt transport, salt crystallization and deformation occurring by shrinkage during initial drying and expansion upon crystallization.

This modelling approach can be used for any kind of porous material (stone, mortar). Validation here is done by a material specifically chosen because of its good properties for crystallization experiments. Further research will include experiments on standard building materials such as bricks, natural stone and mortars.

## References

- [1] Petkovic, J. Moisture and ion transport in layered porous building materials: a Nuclear Magnetic Resonance study, PhD Thesis, T.U.Eindhoven, The Netherlands, 2005.
- [2] Rijniers, L.A. Salt crystallization in porous materials: an NMR study, PhD Thesis, T.U. Eindhoven, The Netherlands, 2004.
- [3] Rucker, P., Holm, A., Krus, M. Determination of moisture and salt content distributions by combining NMR and gamma ray measurements, Materialsweek, Munich, September 2000.
- [4] Koniorczyk, M., Gawin, D. The influence of salt on hygrothermal behaviour of building materials, *Proceeding of the 3<sup>rd</sup> International Building Physics Conference*, Research in Building Physics and Building Engineering, Fazio, Ge, Rao & Desmarais (eds), 2006, 139-146.
- [5] Poupeleer, A.S. Transport and crystallization of dissolved salts in cracked porous building materials, PhD Thesis, K.U.Leuven, Belgium, 2007.
- [6] Coussy, O. Deformation and stress from in-pore drying-induced crystallization of salt. *Journal of the Mechanics and Physics of Solids*, (54), (2006), 1517-1547.
- [7] Coussy, O. *Poromechanics*, Wiley: Chichester, 2004.
- [8] Roels, S., Carmeliet, J. Analysis of moisture flow in porous materials using microfocus X-ray radiography, *International Journal of Heat and Mass Transfer*, (49), (2005), 4762-4772.